Available online at www.sciencedirect.com
SCIENCE DIRECT®
PERGAMON
International Journal of Multiphase Flow 29 (2003) 1565–1581
International Journal of Multiphase Flow
www.elsevier.com/locate/ijmulflow

Multi-holdups in co-current stratified flow in inclined tubes

A. Ullmann, M. Zamir, S. Gat, N. Brauner *

Department of Fluid Mechanics and Heat Transfer, Faculty of Engineering, Tel Aviv University, Tel Aviv 69978, Israel

Received 3 October 2002; received in revised form 17 July 2003

Abstract

Maps of the multi-holdup regions in co-current and countercurrent flows are presented in terms of the controlling non-dimensional parameters. These maps clearly demonstrate the symmetrical relationship between upward and downward co-current inclined flows. The feasibility of obtaining multi-holdups in co-current up flow is validated experimentally using oil–water system. The multiple holdups are shown to be associated with hysteresis phenomenon. The introduction of the multi-holdup regions on flow-pattern maps of various gas–liquid and liquid–liquid systems, indicates that these regions correspond to operational conditions where stratified flow was experimentally observed. The significance of multi-holdups phenomena to transition from stratified flow to other bounding flow patterns is discussed.

Keywords: Co-current; Holdup; Inclined; Multiple; Stratified

1. Introduction

Despite the extensive efforts and the numerous theoretical and experimental investigations into co-current stratified flows in pipes, the issue of multiple holdups attracted a rather limited attention.

Taitel and Dukler (1976, 1986) two-fluid model is widely used as a predictive tool for stratified gas–liquid flows. Baker and Gravestock (1987) and Baker et al. (1988) first pointed out that this model can predict non-unique values of the holdup for given phases flow rates in upward inclined flows. This issue was the subject of a theoretical investigation by Landman (1991). He showed that the multiple holdups in upward stratified flow are not an artifact of the two-fluid model. Similar behavior is predicted by the exact solution for laminar flows in upward inclined square ducts.

* Corresponding author. Tel.: +972-3-640-8127; fax: +972-3-640-7334.
E-mail address: brauner@eng.tau.ac.il (N. Brauner).

0301-9322/$ - see front matter
doi:10.1016/S0301-9322(03)00143-5

According to his stability analysis, the most stable solution is that of the lowest liquid holdup, that of the highest liquid holdup is unstable, while the intermediate holdup can be stable or unstable. This was qualitatively attributed to the lack of backflow in the liquid layer for the case of the lowest holdup. Barnea and Taitel (1992) studied the structural and interfacial stability of the multiple solutions in upward gas–liquid flows. They have concluded that only the solution of the thinnest liquid film is stable, whereas the other two solutions are practically unstable. The common practice in the industry is thus to consider the lowest holdup as the only relevant solution. The non-unique values for the holdup were related only to upward inclined gas–liquid flows, but have never been indicated for downward flows. The present study is focused on the feasibility of obtaining multi-valued holdups in stratified co-current upward and downward flows in gas–liquid and liquid–liquid systems.

In a previous study (Ullmann et al., 2003), the feasibility of obtaining experimentally two different holdups for the same operational conditions in countercurrent flows was demonstrated. The stratified countercurrent flow was also theoretically investigated via the exact solution of two-phase laminar flow between two plates (TP) and the solutions of the two-fluid (TF) model for pipe geometry. Both models confirm the existence of a double-solution for the whole range of feasible countercurrent inclined flows. The models were presented in a unified form that is applicable for both countercurrent and co-current flows. These models are used here to investigate the multiple solutions in co-current flows. Complementary to the theoretical investigation, the experimental phase of this study proves for the first time that also in co-current flows multiple holdups are feasible. At least two different, stable holdups were obtained in liquid–liquid up-flow for the same operational conditions. It is shown that different operational protocol results in different holdups, hence, hysteresis phenomenon is involved.

2. Modeling

The TP model and the TF model, as detailed in Ullmann et al. (2003), are applicable also for the analysis of co-current stratified flows. The flow geometry is schematically described in Fig. 1. The governing equations that are used for the calculation of the holdup are summarized below.

2.1. The two-fluid model

The dimensionless form of the combined momentum equation for the flow in the two layers, which is applicable in the general case of either laminar or turbulent flow in each of the layers, reads:

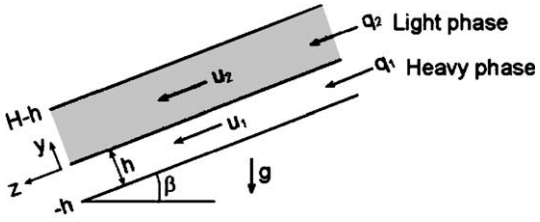

Fig. 1. Schematic description of the stratified flow configuration and coordinates $0 \leqslant \beta \leqslant 90°$.

$$\widetilde{D}_2^{-n_2}\widetilde{U}_2^{2-n_2}\left[\frac{\widetilde{S}_2}{\widetilde{A}_2}+\left|1-q\frac{\widetilde{U}_1}{\widetilde{U}_2}\right|\left(1-q\frac{\widetilde{U}_1}{\widetilde{U}_2}\right)S_i\left(\frac{1}{\widetilde{A}_1}+\frac{1}{\widetilde{A}_2}\right)\right]-\left[\frac{\widetilde{S}_1}{\widetilde{A}_1}\widetilde{D}_1^{-n_1}\widetilde{U}_1^{2-n_1}\right]X^2+4Y=0$$

$$\text{for } \frac{\widetilde{U}_2}{|q|\widetilde{U}_1}>1 \tag{1.1}$$

and

$$\widetilde{D}_2^{-n_2}\widetilde{U}_2^{2-n_2}\frac{\widetilde{S}_2}{\widetilde{A}_2}-\widetilde{D}_1^{-n_1}\widetilde{U}_1^{2-n_1}\left[\frac{\widetilde{S}_1}{\widetilde{A}_1}-\left|\frac{1}{q}\frac{\widetilde{U}_2}{\widetilde{U}_1}-1\right|\left(\frac{1}{q}\frac{\widetilde{U}_2}{\widetilde{U}_1}-1\right)S_i\left(\frac{1}{\widetilde{A}_1}+\frac{1}{\widetilde{A}_2}\right)\right]X^2+4Y=0$$

$$\text{for } \frac{\widetilde{U}_2}{|q|\widetilde{U}_1}<1 \tag{1.2}$$

The dimensionless frictional pressure drop is given by

$$\Pi_f=\frac{(-\mathrm{d}p_f/\mathrm{d}z)}{(-\mathrm{d}p/\mathrm{d}z)_{2s}}=\frac{1}{\pi}[(\widetilde{S}_1\widetilde{D}_1^{-n_1}\widetilde{U}_1^{2-n_1})X^2+\widetilde{S}_2\widetilde{D}_2^{-n_2}\widetilde{U}_2^{2-n_2}] \tag{1.3}$$

In these equations $\widetilde{U}_1=U_1/U_{1s}=\pi/(4\widetilde{A}_1)$ and $\widetilde{U}_2=U_2/U_{2s}=\pi/(4\widetilde{A}_2)$, where U_{1s}, U_{2s} are the superficial phases' velocities. The dimensionless geometrical relationships for the flow areas, wetted perimeters and the interface length, $\widetilde{A}_{1,2}$, $\widetilde{S}_{1,2}$ and $\widetilde{S}_i$ respectively, are given in terms of $\tilde{h}$ for a plane interface (Taitel and Dukler, 1976) and for curved interface in terms of the interface curvature (Brauner et al., 1998). The hydraulic diameters D_1, D_2, are modeled according to the relative velocity of the two layers. The flow characteristics of two-fluid systems are dependent on three dimensionless parameters: the flow rates ratio $q=U_{1s}/U_{2s}$, the inclination and Martinelli parameters, Y and X^2:

$$Y=\frac{(\rho_1-\rho_2)g\sin\beta}{(-\mathrm{d}p/\mathrm{d}z)_{2s}}=\frac{(\rho_1-\rho_2)g\sin\beta}{\frac{2c_2}{D}Re_{2s}^{-n_2}\rho_2U_{2s}|U_{2s}|};\quad X^2=\frac{c_1}{c_2}\frac{Re_{1s}^{-n_1}}{Re_{2s}^{-n_2}}\frac{\rho_1}{\rho_2}|q|q \tag{2}$$

Note that the Martinelli parameter is defined here as the ratio of the superficial frictional pressure gradient for the heavy phase to the superficial frictional pressure gradient for the light phase (not necessarily to that of the less viscous phase, as used in Charles and Lilleleht, 1966; Angeli and Hewitt, 1998). The Re_{1s}, Re_{2s} are the superficial Reynolds numbers of the two phases and the constants $c_{1,2}$ and $n_{1,2}$ are taken according to the flow regime in each of the fluids (e.g. $c=16$, $n=1$ for laminar flows and $c=0.046$, $n=0.2$ for turbulent flow).

In laminar flows the viscosity ratio μ can replace either q or X^2 since $X^2=\mu q$. It was demonstrated in the literature (e.g. Taitel and Dukler, 1976; Brauner and Moalem Maron, 1989) that the holdup predicted by the TF model in terms of these dimensionless parameters is insensitive to the flow regime (laminar or turbulent) in either of the fluid layers.

It is worth emphasizing that the derivation of Eq. (1) uses closure laws for the wall and the interfacial shear stresses that are borrowed from single-phase flow models. These ignore possible effects of the flow geometry and the interaction between the flow in the two layers on the structure and parameters of the closure laws. The weakness of these closure relations in predicting the countercurrent flow characteristics have been demonstrated and discussed in Ullmann et al. (2003).

2.2. The two-plate model

The model assumes laminar flow in both layers and the holdup ($\tilde{h}$) is determined by Y, μ and q by solving the following nonlinear implicit algebraic equation:

$$Y - \frac{1}{4}\frac{X^2(1-\tilde{h})^2[(1+2\tilde{h})\mu + (1-\mu)\tilde{h}(4-\tilde{h})] - \tilde{h}^2[(3-2\tilde{h})\mu + (1-\mu)\tilde{h}^2]}{\tilde{h}^3(1-\tilde{h})^3[\tilde{h} + \mu(1-\tilde{h})]} = 0 \tag{3}$$

where Y is defined by Eq. (3) with $(-\mathrm{d}p/\mathrm{d}z)_{2s} = 12\mu_2 q_2/H^3$ (H denotes the distance between the plates).

Note that co-current flows correspond to positive X^2 with $Y > 0$ for down-flow and $Y < 0$ for up-flow. Countercurrent flows correspond to negative X^2 with $Y < 0$.

3. Prediction of the multiple holdups region

The TP and the TF models described above are used for exploring the range of system parameters where multiple solutions for the holdup are expected in co-current flows.

It was shown in Ullmann et al. (2003) that multiple (double) holdups are inherent in countercurrent flow. However, in co-current flow, multiple (triple) holdups are predicted by the models only in a limited range of operational conditions. For example, Fig. 2 shows the TP model prediction for the variation of the holdup curves as the inclination parameter changes from a negative to a positive value for the liquid/liquid system studied in Ullmann et al. (2003) ($\mu = 1.47$). The triple solution for the upward flow ($Y < 0$) is typically obtained for small positive value of X^2 corresponding to high flow rates of the light phase and/or low flow rates of the heavy

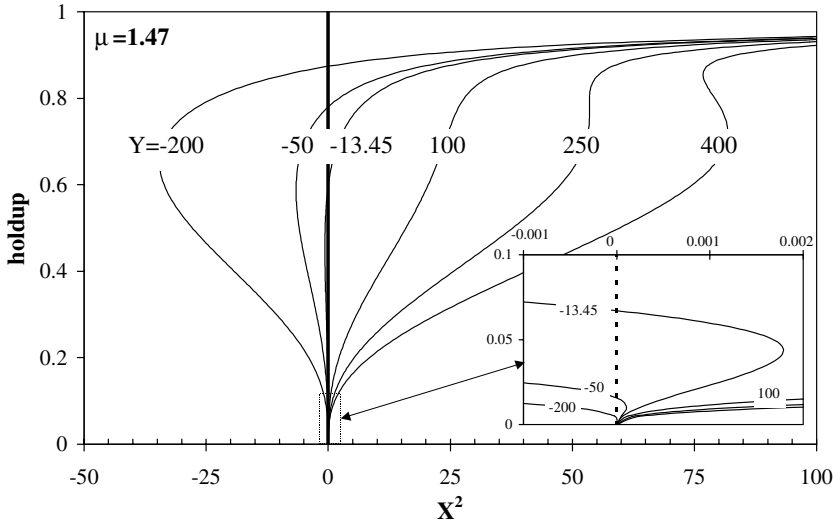

Fig. 2. The effect of the inclination parameter on the holdup curve—demonstration of the triple solutions obtained in co-current upward ($Y < 0$) and downward ($Y > 0$) flows and double solution in countercurrent flows.

phase (see the detailed picture inserted in the figure). This figure clearly shows that triple solutions for the holdup are obtained also in downward flows ($Y > 0$). The triple solutions in downward flows are in the range of relatively high X^2 and correspond to relatively high holdups of the heavy phase. It is worth noting that the similarity between upward and downward flows can be clearly demonstrated by plotting the holdup vs. $1/X^2$ and using Y/X^2 as a parameter for $\mu = 1/1.47$. This would result in a "mirror picture" of Fig. 2.

In view of Fig. 2, for a specified value of Y, the range of X^2 corresponding to multiple solutions is bounded by the values of X^2 corresponding to $\mathrm{d}X^2/\mathrm{d}\tilde{h} = 0$. Using Eq. (3) for calculation of this derivative yields:

$$Y = \frac{\mu^2 - (1 - 2\mu + \mu^2)\tilde{h}^4 + (2 + 4\mu - 2\mu^2)\tilde{h}^3 + (2\mu - \mu^2)\tilde{h}^3}{2\tilde{h}(\tilde{h} - 1)^3((1 - 2\mu + \mu^2)\tilde{h}^4 + (10\mu - 6 - 4\mu^2)\tilde{h}^3 + (4 - 12\mu + 6\mu^2)\tilde{h}^2 + (4\mu - 4\mu^2)\tilde{h} + \mu^2)} \tag{4}$$

Eqs. (3) and (4) can be easily solved simultaneously to yield the X^2 vs. Y relationship that forms the boundaries of multiple solution regions for a given liquid/liquid system: given μ and $\tilde{h}$, Eq. (4) yields Y, and these are then used in Eq. (3) to obtain the corresponding X^2 (or q).

The so-obtained regions of multiple solutions in both co-current and countercurrent flow configurations are summarized in Fig. 3a. The countercurrent flow range ($X^2 < 0$) is associated

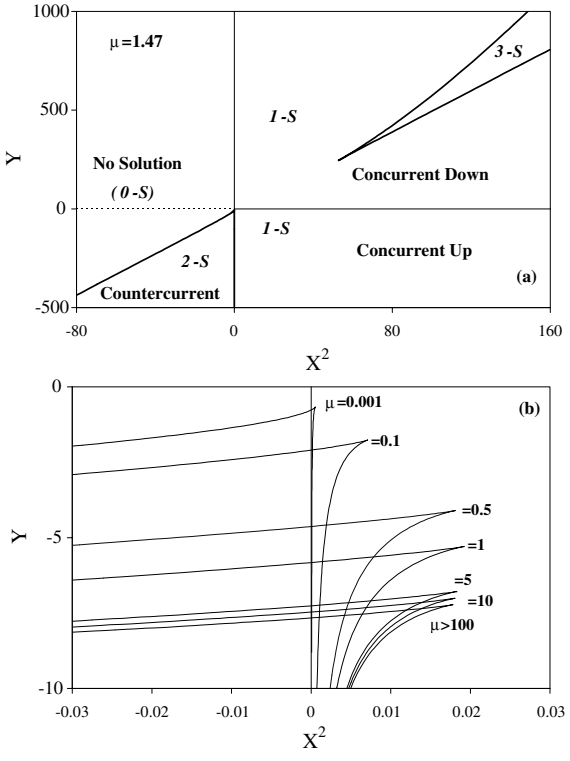

Fig. 3. Multiple-solution regions for co-current and countercurrent flows: (a) $\mu = 1.47$, (b) effect of μ in co-current upward flows.

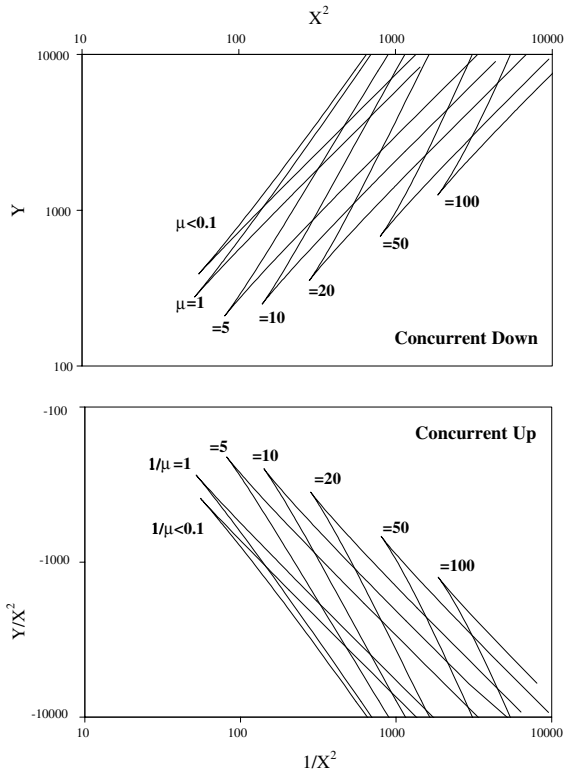

Fig. 4. Multiple-solution regions: the symmetry between the co-current downward and upward flows.

with a double solution for the holdup (2-s). As shown, for any given negative X^2 there is a maximum value of Y for which countercurrent flow is feasible. Co-current flow is feasible in the whole range of positive X^2 (at least 1-s). The triple solution range (3-s) of co-current downward flow is clearly seen in the figure. The range of triple solution for upward co-current flow is for small positive values of X^2 (adjacent to $X^2 = 0$). This region is detailed in Fig. 3b, where the effect of the viscosity ratio on the range of triple solution is demonstrated. The same information for the range of triple solution in upward flow is shown in the lower part of Fig. 4 in terms of Y/X^2 vs. $1/X^2$. The upper part of this figure is actually a mirror image of its lower part and represents the ranges where triple solution exists in co-current downward flows.

Fig. 4 demonstrates the complete similarity between upward and downward co-current flows. It clearly indicates that there is a minimal X^2 (or minimal $1/X^2$) for co-current downward (or co-current upward) flows for which triple solutions can be obtained. This minimal value is about 60 for the range of μ between 0.02 and 1.5 for down-flow (or $1/\mu$ between 0.02 and 1.5 for up-flow). It is interesting to note that for higher μ, in the range of 5–100, the minimal q for obtaining triple solutions in downward flow is approximately constant (about 20, Fig. 5). Figs. 4 and 5 pinpoint the fact that the modeling of the flow in the region of triple solutions requires all the three parameters: X, Y and μ, even in the range of extremely high (or low) viscosity ratios.

The velocity profiles associated with the triple solution of the holdup are demonstrated in Fig. 6 for downward flow. In this case, the lighter phase is dragged downward by the fast moving heavy

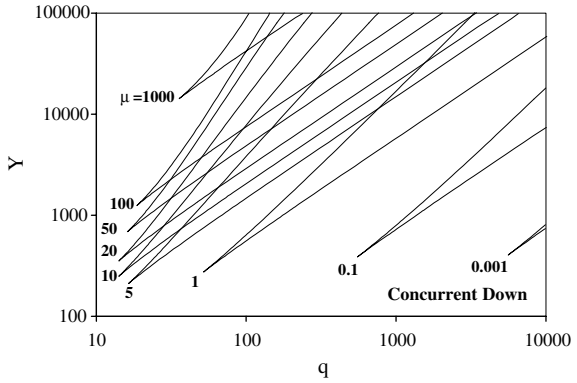

Fig. 5. Multiple-solution regions: the effect of μ on the range of q.

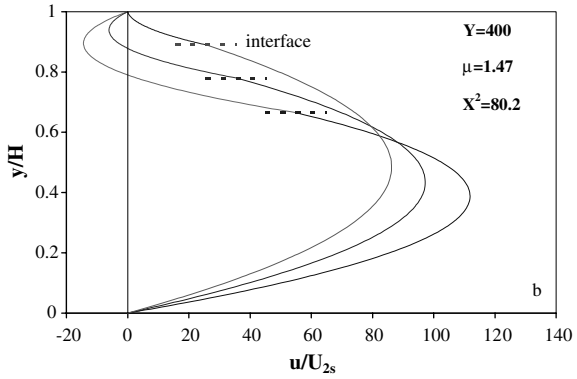

Fig. 6. Velocity profiles associated with the triple-solution holdup curve in downward flow.

phase and the only solution without backflow is that of the highest heavy phase holdup. In the symmetrical upward flow case ($Y/X^2 = -400$, $1/X^2 = 80.2$ and $1/\mu = 1.47$) where the heavier phase is dragged upward by the fast moving light phase, the only solution without backflow is that of the lowest heavy phase holdup. In gas–liquid systems, this solution has been commonly considered as the most stable and thus, the feasible configuration (e.g. Landman, 1991). However, a similar criterion for downward flow, would suggest that the highest heavy phase holdup is the feasible solution. Therefore, the feasible configuration should not be automatically taken as the one with the lowest heavy phase holdup.

From a practical point of view, it is of interest to investigate whether the TP model can be used to identify the range of operational conditions for which triple solutions are expected in pipe geometry. As shown above, the identification of the multiple solution regions via the analytical expressions of the TP model is straightforward. On the other hand, using models for pipe flow for this purpose requires a tedious numerical search. In Ullmann et al. (2003) of this study it has been shown that the TP model can be utilized for the prediction of the holdups in countercurrent pipe flows if the calculations are based on the same superficial velocities in the two geometries

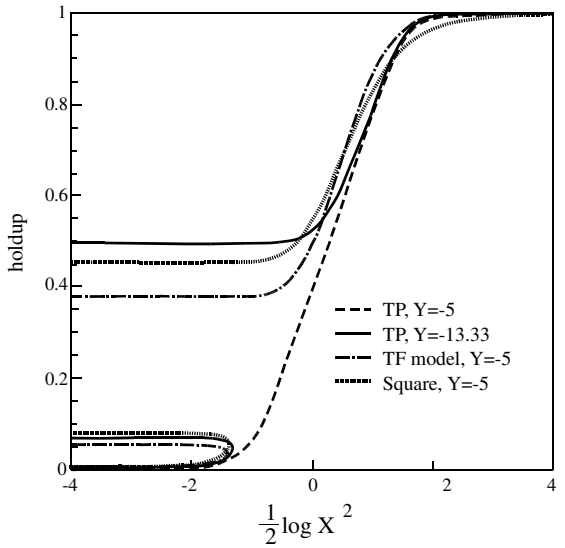

Fig. 7. Comparison between the holdups as predicted by the TP model, the TF model in pipes and the exact solution of Tang and Himmelblau (1963) in a square duct.

(rather than on the same inclination parameter, Y). This implies that the same procedure can be followed for identifying the multiple holdup regions in co-current flows.

The above conjecture is reinforced in view of Fig. 7. The figure shows a comparison between the holdups of co-current up-flow of an air–water system as predicted by the TP model, the TF model for pipe geometry and the exact solution in square duct (Tang and Himmelblau, 1963; Landman, 1991). Indeed, using a value of $Y = -13.33$ in the TP model as equivalent to $Y = -5$ in pipes (equal superficial velocity of the light phase in the two geometries), yields similar prediction by these three models. On the other hand, for $Y = -5$, the TP model dose not yield a triple solution. Note that in all of these models, laminar flow is assumed.

The use of the TP model for indicating the location of the triple-solution region on flow pattern map for laminar–laminar (L–L) pipe flow and for other flow regimes is elucidated with reference to Fig. 8a. This figure corresponds to air–water flow in a 2° upward inclined pipe. The following procedure is applied:

(a) Assuming laminar flow in both the gas and liquid layers (L_G–L_L), the boundaries of the triple-solution (3-s) region, as obtained via the *TP model* in terms of Y vs. X^2 (see Fig. 4), can be transformed to obtain the corresponding boundaries in terms of U_{GS} vs. U_{LS} for a particular system. The same U_{GS} vs. U_{LS} relation applies to pipe geometry. This yields boundary 1 in Fig. 8a.
(b) The Reynolds numbers on boundary 1 (based on the phases' actual velocities and hydraulic diameters) are calculated. If these correspond to L_G–L_L, boundary 1 is the predicted 3-s region in pipe flow. Otherwise, calculate the Y vs. X^2 relationship for L_G–L_L *pipe flow* using the values of U_{GS} vs. U_{LS} along boundary 1 and proceed to the following step.

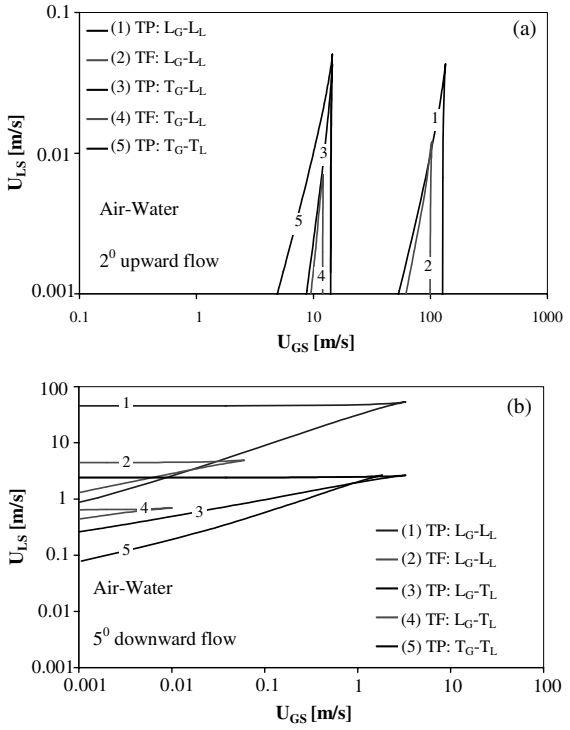

Fig. 8. Multiple-solution regions: presented on a flow pattern map the use of the TP model for the prediction of 3-s regions for flow regimes other than L–L flow: (a) upward flow, (b) downward flow.

(c) Based on the insensitivity of the TF model predictions to the flow regime (when the dimensionless parameters, Y and X^2 are used), the above Y vs. X^2 values obtained in (b) are assumed to represent the boundaries of the 3-s region also in cases of turbulent (T) flow in either one of the phases or in both (T_G–L_L, L_G–T_L, T_G–T_L). Accordingly, these Y vs. X^2 values are used to calculate the corresponding U_{GS} vs. U_{LS} according to the valid flow regime. For instance, this procedure yields boundary 3 in Fig. 8a for the case of T_G–L_L. Similarly, boundary 5 is obtained for the case of T_G–T_L, which is valid only for relatively high liquid flow rates (at the upper part of the multiple solution region).

The 3-s regions as predicted by the TF model for L_G–L_L and T_G–T_L pipe flows are also shown in Fig. 8a, boundaries 2 and 4 respectively. The TF 3-s regions are practically enclosed within the corresponding regions obtained via the TP model and the above procedure. The same procedure is followed for identifying the 3-s regions in co-current downward flow (Fig. 8b). Note however that the identification of the 3-s regions of the TF model required tedious searches, whereas the application of the analytical expression of the TP model for this purpose (Eq. (4) with the above procedure) is straightforward and significantly easier. The similarity between the TF 3-s regions and the corresponding regions obtained via the TP model substantiates the validity of the suggested procedure of using the laminar TP model for estimating the 3-s regions in pipe flows for different flow regimes in the two layers. This similarity implies that the underlying assumption of

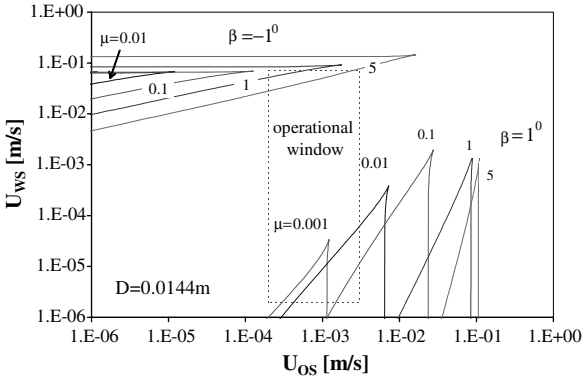

Fig. 9. Variation of the 3-s regions of water–oil system with the viscosity ratio for upward ($\beta > 0$) and downward ($\beta < 0$) flows.

the holdup predictions being insensitive to the flow regimes, once obtained for the same dimensionless parameters (Y, X^2 and q), applies also to the multiple solution regions.

Following the above discussion, the question that arises is whether multiple holdups in co-current stratified flows are feasible in reality, or are just artifacts of the mathematical models. In the latter case, only a single configuration can be obtained for particular operational conditions. In Ullmann et al. (2003), it has been shown that in liquid–liquid countercurrent flow, the two configurations that are predicted by the model are experimentally obtained. It is therefore of interest to explore experimentally co-current flows in the region where multiple holdups are predicted by the model.

The first stage was to identify an appropriate two-fluid system for which the predicted 3-s region matches the operational window of the experimental setup in our laboratory (see Ullmann et al., 2003). Taking water as one of the fluids ($\mu_1 = \mu_w = 1$ cP), the variation of the 3-s region with the viscosity ratio ($\mu = \mu_1/\mu_2$) is demonstrated in Fig. 9 for upward ($\beta = 1°$) and downward (denoted by $\beta = -1°$) co-current flows. For upward flow the highest and widest range is obtained for $\mu \approx 0.1$ where laminar oil and water flows (L_o–L_w) prevail. The effect of inclination on the location of the 3-s for this viscosity ratio ($\mu = 0.1$) is shown in Fig. 10. The figure implies that the

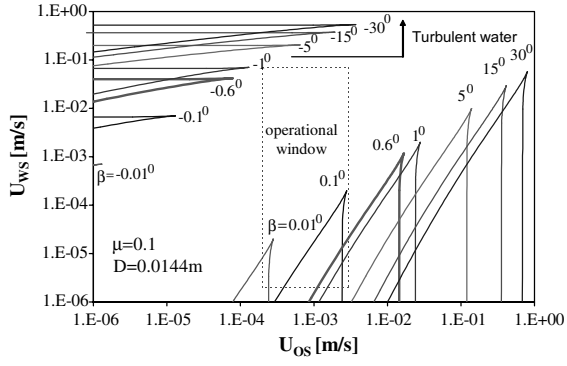

Fig. 10. Variation of the 3-s regions of water–oil system with the inclination for downward ($\beta < 0$) and upward ($\beta > 0$) flows.

3-s region can be obtained within the operational window for $0.01° < \beta < 1°$. Applying Kelvin–Helmholtz (K–H) stability analysis (Brauner and Moalem Maron, 1992) indicates that in this range the three predicted holdups are stable. It is worth noting that for downward flow, the stable 3-s region is practically out of the operational window of the experimental setup.

4. Experimental

4.1. Experimental setup

The experimental setup is similar to that presented in Ullmann et al. (2003). The liquids are fed co-currently (instead of countercurrently) to the test column consists of a one-meter length, 14.4-mm I.D. Pyrex pipe (Duran) with wall thickness of 1.8 mm. The liquid system has been carefully selected so that the operational conditions where multiple holdups are predicted would be within the operational window of the experimental setup. According to the above analysis (Figs. 9 and 10), the liquids used are water and mineral oil (MARCOL 52) with a dimensionless density contrast of $\Delta\rho/\rho_w = 0.165$, viscosity ratio of $\mu = \mu_w/\mu_o = 0.103$ and surface tension $\sigma \approx 0.032$ N/m (at room temperature). The corresponding Eotvos number of the system, $Eo = \Delta\rho g D^2/\sigma \approx 10$, is smaller than that of the solvents system used previously (Ullmann et al., 2003), hence capillary and wall wetting effects may play a role. Since the pipe is hydrophilic, all experiments were started with water in the pipe in order to minimize hysteresis due to wetting effects (see Fig. 13 below). The maximal Reynolds number of the liquids was below 100.

The location of the interface and the corresponding holdup was measured using the same technique that is described in Ullmann et al. (2003). In order to verify the establishment of fully developed conditions, measurements were taken at several locations along the middle section of the pipe (30 cm apart from each side). In all cases, only random variations of the holdup were observed (within the measurement error range, less than 3%). Likewise, the visualization of the flow field and the local velocity measurements (PIV) were also applied to the co-current flows. Further details can be found in Gat (2002).

4.2. Experimental results

Fig. 11 shows the experimental results for the water holdup obtained in the pipe inclined upward by 0.6°. In this experiment, the oil flow rate was maintained constant ($Y = -4.81$), while the water flow rate (q_1) was varied in the range where triple solutions of the holdup are anticipated. Starting with low flow rate of water and introducing co-current flow of oil (low X^2), results in a thin water layer. However, a slight increase of the water flow rate, results in an abrupt change of the water holdup to values, which are about six times higher. With a further increase of the water flow rate, a mild increase of the holdup was observed. Going on the other direction by reducing the water flow rate, practically the same holdups were obtained, except in the range of low water flow rates. Here, as $q_1 \to 0$, the water holdup maintains the higher level of about 0.35, and the low holdups of 0.07 were not reached. Moreover, the situation of single-phase oil flow was not recovered for zero water flow rate. Under this condition, the zero water flow rate is associated

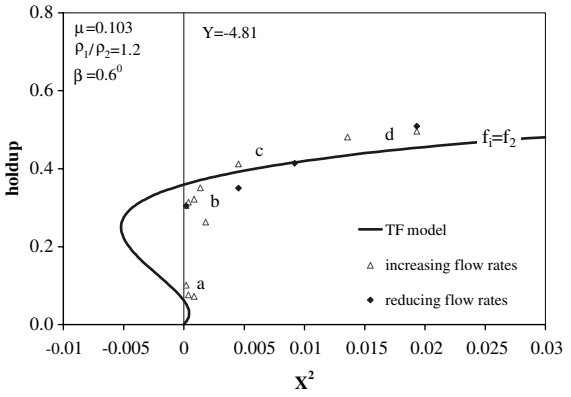

Fig. 11. Experimental evidence for the existence of multiple holdups in co-current upward flow for: $Q_2 = -23$ ml/min, $\mu_2 = 9.7 \times 10^{-3}$ kg/m/s, $\rho_2 = 835$ kg/m^3 corresponding to $Re_{2s} \approx 3$.

with a complete circulation in the water layer. The hysteresis loop so obtained (a–b–c–d–c–b), results in two different holdups, which are obtained for the same water flow rate (multiple holdups). This experiment validates the feasibility of obtaining multiple holdups and these are not artifacts of the models.

The results of the TF model for the experimental conditions are also shown in Fig. 11. Note that, in upward co-current flow, the TF model with curved interface (Brauner et al., 1998) is applied with $f_i = f_2$, as the heavier water phase is dragged upward by the oil phase. As shown, the model predicts the multiple holdups and the hysteresis loop. The experimental lower holdup (a) seems to be associated with the 'middle' model solution. If this is the case, it is the lower solution (of an extremely low holdup) that was not detected in the experiment. The TF model (as well as the TP model) indicates that a continuous backward path from (b) to (a) is feasible only through the countercurrent flow region. It is of interest to note at this point that stability analysis indicates that all the three possible solutions are stable. This will be further discussed in the next section.

The velocity profiles in both of the phases obtained by the PIV method are shown in Fig. 12 for the conditions associated with points a, b and d in Fig. 11. The corresponding velocity profiles predicted by the TP model for the same conditions are shown on the R.H.S of the figure (although the middle point (b) holdup is overestimated). The TP model predicts backflow in the heavy phase in the 'middle' (b) and the 'upper' (c) holdups, as well as at point (d). The backflows associated with points (b) and (d) are validated experimentally. However, the slight backflow predicted by the TP model for point (a) was not observed.

Complementary to Fig. 11, the predictions of the holdup by the TF and TP models are examined by comparison with experimental data obtained at water-cut of 50% and various shallow (0–3°) upward inclinations (Fig. 13). Here too, the TP model is applied using the same superficial velocities as in pipe flow (denoted in the figure by equal Us). Note that in the TP model the holdup is given by $\tilde{h}$. The two models predict the sensitivity of the holdup to a slight off-horizontal inclination, and generally, follow the increase of the holdup with the inclination. Note that the data of Fig. 13 was obtained with initial wetting of the pipe with water. In this case repeatable results were obtained independently of the direction of the inclination change (and the corresponding

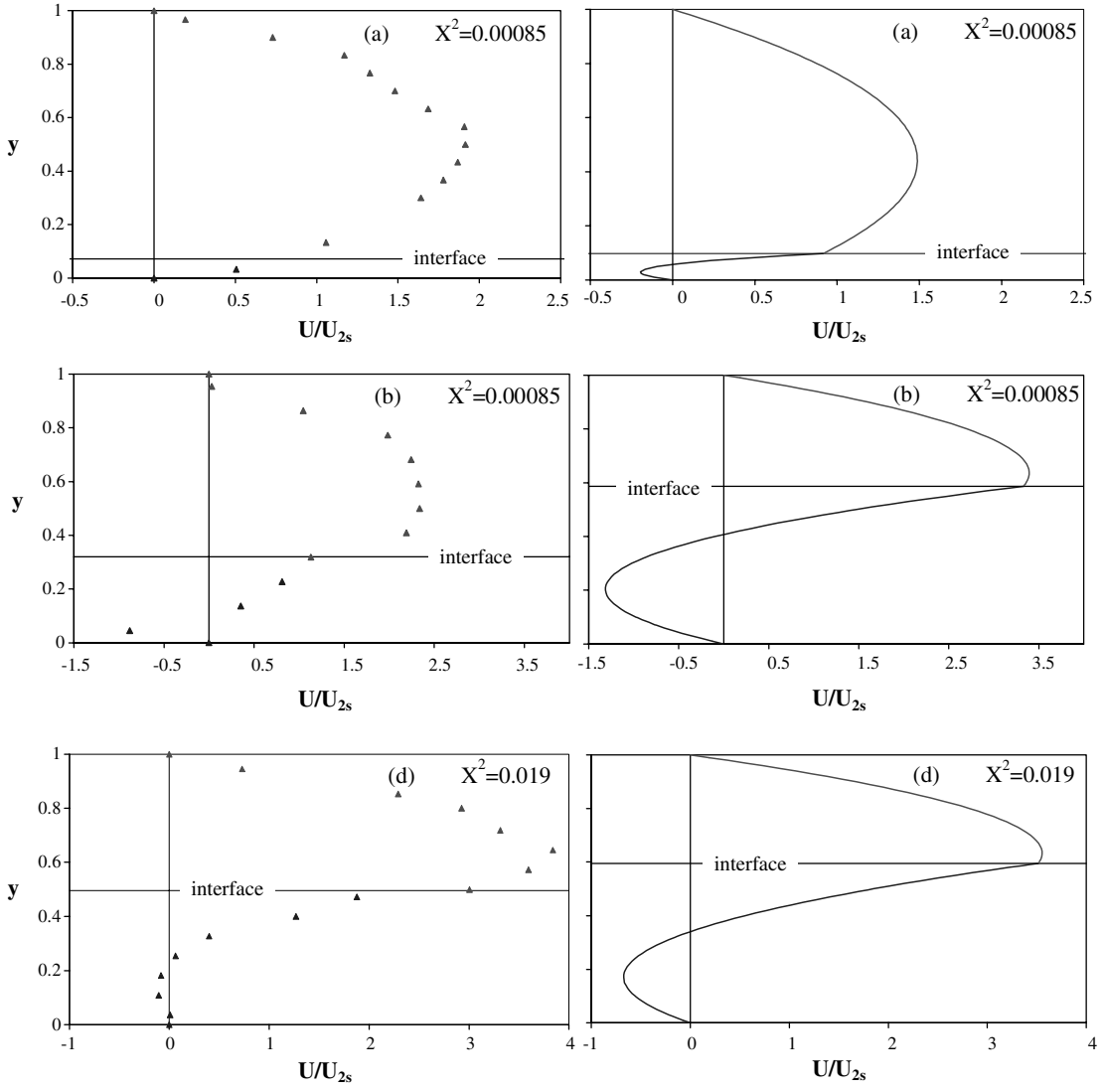

Fig. 12. Measured velocity profiles for conditions associated with point a, b (multiple holdups) and d of Fig. 11: (left column) compared to the prediction of the TP model (right column).

direction of holdup variation). On the other hand, hysteresis related to wetting effects was observed when the pipe was initially wetted by the oil (Gat, 2002).

5. Implications of 3-s regions to flow pattern transitions

Following the experimental validation of the existence of multiple holdups, it is of interest to examine the stability of the three solutions. To this aim, the linear stability analysis of the

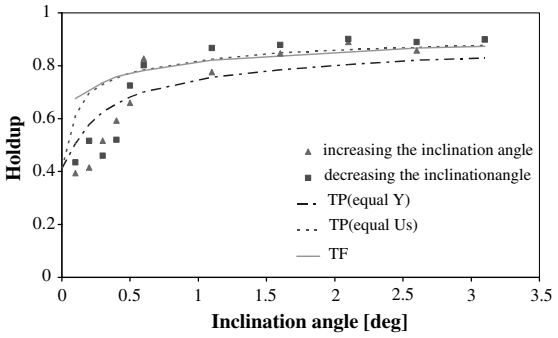

Fig. 13. Effect of the pipe inclination on the holdup: comparison of experimental results with the prediction of the TP and the TF models; $Q_1 = -13$ ml/min; $Q_2 = -11$ ml/min; $\mu_2 = 0.0097$ kg/(m s); $\rho_2 = 835$ kg/m^3 corresponding to $Re_{1s} \approx 1.4$; $Re_{2s} \approx 1.6$.

transient TF model is applied (Brauner and Moalem Maron, 1992; Brauner, 1998). This analysis indicates that for the case of 0.6° upward inclined pipe, all the three solutions for the holdup are stable throughout the 3-s region. It is worth emphasizing that a full K–H stability analysis, which considers the inertia of both the water and oil phases is required, as both are of the same order of magnitude. Fig. 14 shows the location of multiple solutions regions (as predicted by the TF and

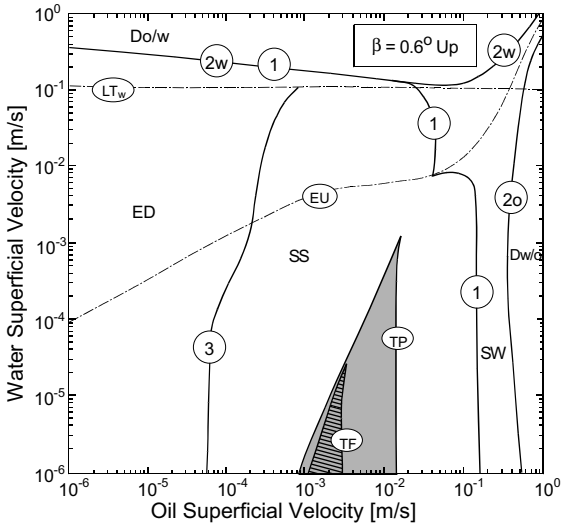

Fig. 14. The location of the multiple solution regions (as predicted by the TP and the TF models) on the stratified flow stability map as predicted by linear stability analysis (Brauner and Moalem Maron, 1992; Brauner, 1998), $\mu_{oil} = 0.0097$ kg/(m s) $\rho_{oil} = 835$ kg/m^3. Flow pattern notation: ED—elongated oil drops, SS/SW—stratified smooth/wavy, Do/w, Dw/o—dispersion of oil in water, water in oil. Boundaries notation: 1—neutral stability boundary for SS, 2—well-posedness boundary (2o—faster oil layer, 2w—faster water layer), 3—transition from SS to ED, EU—equal velocity of the oil and water layers, LTw—laminar/turbulent transition in the water layer, TP, TF—triple solution boundaries in the corresponding models.

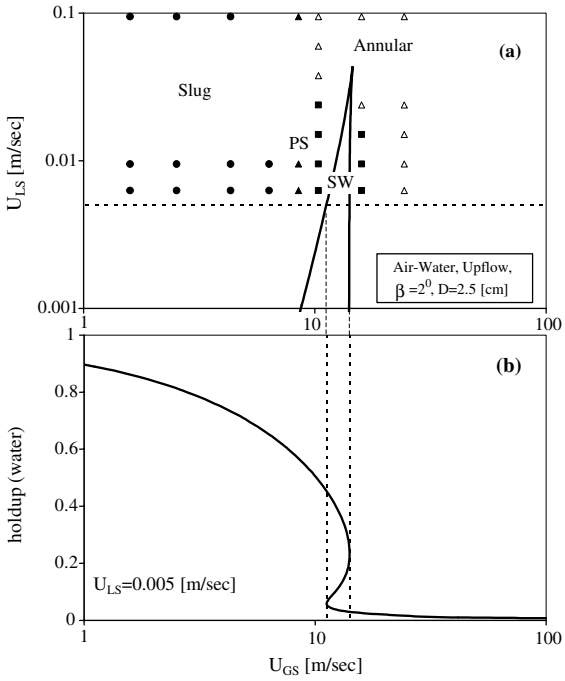

Fig. 15. (a) The triple-solution region indicated on a flow pattern map for upward flow of an atmospheric air–water system. Experimental flow pattern data, Barnea and Taitel (1986), (b) the variation of the holdup as obtained by the TP model. ■ Stratified wavy (SW), ● slug, ▲ pseudo slug (PS), △ annular.

TP models) on the stratified flow stability map. As shown, the 3-s region corresponds to laminar flow in both phases, and is located within the larger region where stratified flow is predicted to be stable (inside boundary 1). Therefore, in this particular system, the 3-s region is not associated with the location of flow pattern transition. In other systems, however, the drastic change in the holdup characterizing the 3-s region (and its vicinity) may correspond to the locus of flow pattern transition.

For example, Fig. 15a shows the region where stratified flow is experimentally observed in upward inclined air–water system. This region almost coincides with the predicted 3-s region, and this is not a coincidence. The sequence of flow patterns observed when the air flow rate is increased at a constant water flow rate (e.g. $U_{LS} = 0.005$) is slug flow, stratified flow and then transition to annular flow. The associated variation of the holdup as obtained by the TP model (following the procedure outlined in Section 3) is shown in Fig. 15b. Left to the 3-s region, the stratified flow model yields a single solution of relatively high water holdup, which is unstable according to K–H criterion (Brauner and Moalem Maron, 1992). Indeed, slug flow is observed in this region. As the 3-s boundary is reached, an additional, low holdup solution suddenly appears. Stability analysis of this solution suggests stratified wavy flow (Brauner and Moalem Maron, 1993, 1994), which is also observed experimentally. At higher gas flow rates, drops entrainment from the wavy interface results in a gradual transition to annular flow. From the practical point of view, in this upward inclined air–water system, the left boundary of the 3-s

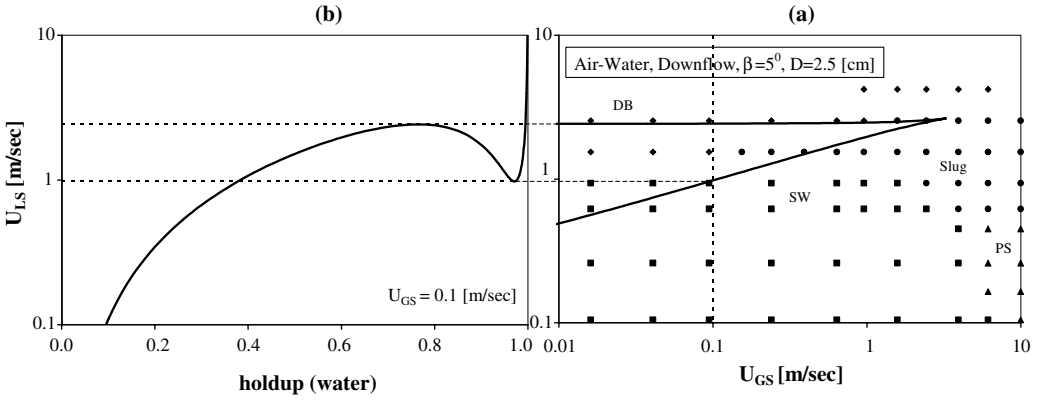

Fig. 16. (a) The triple-solution region indicated on a flow pattern map for downward flow of an atmospheric air–water system, experimental flow pattern data, Barnea and Taitel (1986), (b) the variation of the holdup as obtained by the TP model. ■ Stratified wavy (SW), ● slug, ◆ dispersed bubbles (DB), ▲ pseudo slug (PS).

region coincides with the locus of flow pattern transition. Moreover, in the 3-s region, all the solutions should be considered while performing stability analysis of the stratified flow configuration.

A similar situation may occur in downward inclined systems. This is shown in Fig. 16a for the case of air water down flow in a 5° inclined tube. Also in this case, the predicted 3-s region is at the vicinity of the experimentally observed transition between stratified and slug flow. In down-flow, the 3-s region corresponds to an abrupt change of the water holdup from very high values (where slug flow is observed) to lower values where stratified wavy flow prevails (see Fig. 16b).

6. Conclusions

In our recent study (Ullmann et al., 2003) we have shown that in countercurrent flows multi (double) solutions are predicted theoretically, and can be obtained experimentally. In this part, we have proven experimentally that multiple holdups also exist in co-current inclined flows.

Multi-holdups are obviously associated with multi-value pressure drops and other flow characteristics. Therefore, in the range of operational conditions where multiple solutions are suspected, the modeling and design of two-phase flow systems should be approached with extra care. Computational codes usually provide only one solution for specified operational conditions. Therefore, it is necessary to make sure that this solution indeed corresponds to the relevant, physical configuration. Moreover, the possibility of other feasible configurations should be examined.

A simple procedure, which is based on the analytical solution of laminar flow between two-plates, is established for identifying the regions where multiple holdups are suspected in co-current flows. This procedure avoids the tedious search required by other models for identifying these regions.

Mapping the multiple-holdup regions clearly show the existence of a complete similarity between upward and downward co-current inclined flows. The locations of these regions on the flow

pattern maps imply that the conditions associated with multi-valued holdups are of special significance for the transition from stratified flow to other bounding flow patterns.

It is worth noting, that the commonly used two-fluid model may fail in indicating the multiple holdup regions due to problematic modeling of the interfacial and wall shear stresses in inclined flows. This is probably the reason that the possibility of obtaining multi-valued holdup in downward flows has not been discussed so far in the literature.

References

Angeli, P., Hewitt, G.F., 1998. Pressure gradients in horizontal oil–water flow. Int. J. Multiphase Flow 24, 1184–1203.

Baker, A., Gravestock, N., 1987. New correlations for predicting pressure loss and holdup in gas/condensate pipelines. In: Proceedings of the Third International Conference on Multiphase Flow, The Hague, The Netherlands, pp. 417–435.

Baker, A., Nielsen, K., Gabb, A., 1988. Pressure loss, liquid holdup calculations developed. Oil Gas. J. (March 14), 55–59.

Barnea, D., Taitel, Y., 1986. Flow pattern transition in two phase gas–liquid flows. In: Chermishinof, N.P. (Ed.), Encyclopedia of Fluid Mechanics. Gulf, Houston, TX, pp. 403–474.

Barnea, D., Taitel, Y., 1992. Structural and interfacial stability of multiple solutions for stratified flow. Int. J. Multiphase Flow 18, 821–830.

Brauner, N., 1998. Liquid–liquid two phase flow in HEDU, Heat Exchanger Design Update-section 2.3.5, Begell House, New York, 1998.

Brauner, N., Moalem Maron, D., 1989. Two-phase liquid–liquid stratified flow. Physico-Chem. Hydrodynam. 11, 487–506.

Brauner, N., Moalem Maron, D., 1992. Flow pattern transitions in two-phase liquid–liquid horizontal tubes. Int. J. Multiphase Flow 18, 123–140.

Brauner, N., Moalem Maron, D., 1993. The role of interfacial shear modeling in predicting the stability of stratified two-phase flow. Chem. Eng. Sci. 8 (10), 2867–2879.

Brauner, N., Moalem Maron, D., 1994. Dynamic model for the interfacial shear as closure law in two-fluid models. Nuclear Eng. Des. 149, 175–183.

Brauner, N., Rovinsky, J., Moalem Maron, D., 1998. A two-fluid model for stratified flows with curved interfaces. Int. J. Multiphase Flow 24, 975–1004.

Charles, M.E., Lilleleht, L.U., 1966. Correlation of pressure gradients for the stratified turbulent-laminar pipeline flow of two immiscible liquids. Can. J. Chem. Eng. 44, 47–49.

Gat, S., 2002. Two-phase liquid–liquid co-current flow in inclined tubes, M.Sc. Thesis, Faculty of Engineering, Tel-Aviv University, Israel.

Landman, M.J., 1991. Non-unique holdup and pressure drop in two-phase stratified inclined pipe flow. Int. J. Multiphase Flow 17, 377–394.

Taitel, Y., Dukler, A.E., 1976. A model for predicting flow regime transitions in horizontal and near horizontal gas–liquid flow. AIChE J. 22, 47–55.

Taitel, Y., Dukler, A.E., 1986. Flow pattern transitions in gas–liquid flow: measurements and modeling. In: Multiphase Science and Technology, vol. 2. Hemisphere, Washington, DC, USA.

Tang, Y.P., Himmelblau, D.M., 1963. Velocity distribution of isothermal two-phase co-current laminar flow in a horizontal rectangular duct. Chem. Eng. Sci. 18, 143–148.

Ullmann, A., Zamir, M., Ludmer, Z., Brauner, N., 2003. Stratified Countercurrent Flow of Two Liquid Phases in Inclined Tubes. Int. J. Multiphase Flow, doi:10.1016/S0301-9322(03)00144-7.